Surface-enhanced Raman scattering spectra of radial breathing and G band modes in functionalised nanotubes

Nebras Al-Alttar [1], Ilona Kopf [2], Kevin Flavin [2] , Eamonn Kennedy [1], Silvia Giordani [2], James H Rice [1]

[1] *School of Physics, University College Dublin, Belfield, Dublin 4, Ireland*
[2] *School of Chemistry/CRANN, Trinity College Dublin, Dublin 2, Ireland*

Corresponding author
James Rice
School of Physics, University College Dublin
Belfield, Dublin
Ireland
Email: james.rice@ucd.ie
Phone: 00353 1 1762229

Key words
carbon nanotubes, surface enhanced Raman, chemical modification

Abstract

In this paper we perform surface enhanced Raman scattering studies of two functionalised nanotubes, an oxidised SWCNT and a SWCNT with a fluorescein side group covalently attached to the nanotube was compared with pristine SWCNTs. Our studies showed that in the G- band a significant shift was seen, while relatively little change occurred in the G+ and RBM spectral regions. These results indicate that SERS is broadly in line with Raman studies of chemically altered SWCNTs.

1. Introduction

Considerable amount of research has been undertaken to advance the understanding of optical processes in nanomaterials such as quantum dots, nanodisks, fullerenes and carbon nanotubes [1-11]. Single-walled carbon nanotubes (SWCNT) are one class of nanomaterial that has attracted considerable research effort in understanding and applying their properties [1,2]. One of the challenges in applying SWCNTs to create devices is that these nanotube structures form metastable suspensions rather than true solutions. One way to overcome this is functionalization of the SWCNT [12-20]. Functional groups covalently attached to the nanotube sidewalls prevent the aggregation of SWNTs into bundles and enhance their solubility/dispersibility in organic solvents. The addition of a chemical group via covalent bonding alters the conjugative network of the graphene sheet and creates changes in the electronic structure of the SWCNT. In addition to this the exposure to chemical treatments potentially results in the displacement of carbon atoms from graphite network creating vacancies [21-23]. Localization of electronic density around these defects have been shown to improve such properties as field emission, chemical detection sensitivity and electrochemical capacity as well as interface interactions between the nanotube surface and materials [1,2].

Surface enhanced Raman spectroscopy (SERS) is a well-established technique that enables measurements of the structure of SWCNTs. The use of a rough metallic substrate with a roughness in the nm range enables surface plasmons to electromagnetic enhance the Raman signal via coupling of the surface plasmon polaritions to the dipole of the SWCNT [24-30]. In addition to this electromagnetic enhancement mechanism a chemical enhancement mechanism can occur which takes account of the chemical nature of the SERS active substrate and the probe SWCNT molecule. Charge transfer processes can take place between the metallic substrate and adsorbed SWCNT molecule [1,31,32]. The morphology of the metal substrate is an important parameter. It is reported that the surface chemical reactions involve only few molecular layers, while the penetration depth of the surface electromagnetic wave associated to the surface plasmons is much larger, this results in the selection of film thickness been potentially a significant parameter in SERS studies [31-33].

Altering the properties and functionality of SWCNTs through the addition of covalently bounded molecular groups is a well-developed technology [12-20]. Raman spectroscopy (including SERS) provides a potential method to characterise functionalised SWCNTs. Radial breathing mode (RBM) peak shift in the Raman spectrum has been reported to be a method of characterising SWCNT functionalization [34,35]. Mevellec et al studied SWCNTs covalently functionalized according to two processes (esterification and reductive alkylation yielding two classes of functional groups attached to the nanotube) using Raman spectroscopy [34]. A shift in RBM frequencies after functionalization of typically 3 to 4 cm^{-1} for carbon chains and 7 to 8 cm^{-1} for ester groups attached to the nanotube was reported. The ester group possessing oxygen positioned close to the tubes surface. This is interpreted as a result of electron transfer where the oxygen been more electronegative than carbon thereby perturbing the nanotubes electronic structure to a greater degree.

SERS enables significant enhancement in the Raman scattering cross section from analytes supported on carefully chosen plasmon active substrates. This enables Raman to apply to analyse lower concentrations than standard Raman would otherwise enable. However SERS from SWCNTS is known to be sensitive to the nature of the substrate and excitation

wavelength. Studies of SWCNTs on thin silver films of 10 nm can lead to spectral features assigned to partial degradation of carbon nanotubes via nanotube-metal substrate interface, leading to the formation of graphite-like or carbon particles as indicated by the presence of Raman bands of amorphous carbon together with new bands of C_{60}-like molecules [33]. The presence of showing Raman bands of amorphous carbon together with new bands of C_{60}-like molecules. SERS studies of SWCNTs with covalently added molecules have been less studied compared to Raman spectroscopy studies. SERS studies of fluorinated SWCNTs created using F_2 showed that a decrease in intensity of the RBM and an increase in intensity of the D-band occurs [35-38] due to the formation of covalent bonds C–F on the nanotube sidewalls. Here we outline SERS studies of two functionalised nanotubes, an oxidised SWCNT and a SWCNT with a fluorescein side group covalently attached to the SWCNT. SERS studies were performed at two different wavelengths, one in resonance with metallic and a second wavelength in resonance with semiconductor nanotubes.

In this paper we assess the impact of the substrate on the SWCNTs SERS spectral features assessing these features for signatures of the formation of amorphous carbon together with and/or C_{60}-like molecules. We examine the SERS spectra of oxidised SWCNTs and SWCNTs with covalently bonded side groups assessing the differences between these nanotubes in the RBM and G band region in order to better understand the effects that covalently attaching functional groups to the nanotube has on SERS spectral features.

2. Experimental

SERS measurements were carried out with a single monochromator (Roper Acton SP2300s) and EMCCD (Andor IXON) in a backscattering configuration using a 40× objective to excite and collect the scattered light. The spectral resolution was >1.5 cm^{-1}. SERS measurements were conducted with 532 nm (Nd:YAG laser) and 632 nm (HeNe) excitation. The SERS substrates consisted of a thin film of silver of 22 nm in thickness which was deposited onto a glass slide using thermal vacuum deposition. This created the SERS active support onto which the SWCNTs were deposited. SWCNTs were dispersed at low concentration in ethanol (abs) by sonication spray coated onto freshly prepared SERS substrates and dried in a desiccator.

Raw HiPco SWCNTs (p-SWCNT) were purchased from Unidym, Inc. (Lot No. R0513). Highly purified and selectively oxidized SWCNTs (o-SWCNTs) were prepared according to a recently published protocol [14,19]. Briefly, purification/oxidation involves a short nitric acid oxidation to minimize structural/electronic degradation of SWCNTs and sodium hydroxide treatments to remove carboxylated carbonaceous impurities. A hydrogen peroxide oxidization step efficiently etches remaining carbonaceous impurities and ensures full oxidation of oxygenated species to carboxylic acid moieties. Persistence of characteristic optical properties indicating the preservation of the electronic structure during chemical treatment has been demonstrated [14]. Purified and oxidized SWCNTs were covalently functionalized with benzoic acid groups [39,40] and finally a fluorescence probe, fluoresceinamine, was coupled to the benzoic acid groups (f-SWCNT).

3. Results and discussion

The silver substrate film (shown in Fig 1) was examined by AFM [41]. An inhomogeneous surface topography was found. Certain regions of the sample surface are rough on the order of 100’s of nm and others reveal a roughness on the scale of 10’s of nm. ‘Hot spot’ areas of

high plasmon enhancement may be present on this sample as a result of the fragmentation of the silver, in addition to roughed surface features created as a result of the presence of silver nanoparticles. Studies of nanotubes dispersed onto a glass substrate were undertaken using AFM. The sample shows the presence of aggregates on the sample surface containing few nanotubes. The presence of single nanotubes was not definitively found due to a combination of the small size of these structures making it difficult for the AFM to image them. Images of the carbon nanotubes were obtained on a cleaned glass slide to determine their dispersion, whereby the glass forms a smooth surface. The distribution of the nanotubes was seen to be inhomogeneous across the sample surface. The presence of aggregates of nanotubes and the inhomogeneous distribution of silver on the substrate indicates that there is expected to be a variation in the Raman spectral features expected when probing a small area of the sample. The use of a high powered objective (ie 60X) enables the probing of areas of the sample on the few micron length scales. The optical absorption spectrum of the substrate (shown in fig 1) shows a broad absorption band. This absorption band is in resonance with both 532 and 633 nm excitation wavelengths resulting in surface enhancement of the SWCNTs.

SERS spectra of o-SWCNT and f-SWCNT were recorded on a silver substrate surface (shown in Fig 2). The SERS spectra shown in Fig 2 possess spectral features associated with SWCNT. The spectra show features at c.a. 1590 cm^{-1} which are assigned to the G band region and a band at c.a. 1330 cm^{-1} assigned to a the D band region of SWCNTs. The observed SERS spectra is modified compared to the Raman spectra for both the o-SWCNT and f-SWCNT as evidenced by the large D band SERS intensity compared to the spectral features for the Raman spectral features [14]. The intense D band in the SERS indicates a change in the degree of disorder. The D band in the SERS increases its intensity and displays a change in profile. The broadening of the D and G band region has been assigned to an interaction between the silver and the nanotube centering on the charge transfer mechanism responsible (in part) for the SERS enhancement [33]. The presence of the silver nanoparticle layer potentially contributes also to this broadening and enhancement of the D band region.

SERS spectra in the RBM region were recorded. Fig 2 shows the SERS spectra for o-SWCNT and f-SWCNT recorded at 532 and 632 nm for the RBM region. The RBM spectra recorded at 532 nm for o-SWCNT and f-SWCNT possess similar spectral profiles with a large background present. Each spectra was recorded at the same excitation power of 10 mw before the objective. The RBM spectra recorded at 632 nm shows a much lower background and more clearly defined peaks. The RBM frequency of SWCNTs is inversely proportional to tube diameter. The tube diameter can be calculated according to $\omega_{RBM} = 248/d_t$, where ω_{RBM} and d_t indicate the RBM frequency and tube diameter, respectively [1]. Maultzsch et al applied resonant Raman to study the RBM modes of nanotubes for more than 50 chiral indices with diameters between 0.6 and 1.5 nm [35]. The authors noted that $\omega_{RBM} = 248/d_t + C$ is required to account for additional external forces, e.g., from interactions with a substrate or neighbouring tubes in a bundle. The silver SERS active potential creates additional external forces on the nanotube thus requiring correction for estimation of the ω_{RBM}, however it is noted that changes in the environment of the tubes probed so far lead to negligible changes in the RBM frequencies due for few number of tubes in the bundle .

Fig 3 shows a SERS spectrum of p-SWCNT recorded on a 22 nm silver film in the RBM band region recorded at 632 nm with a resonance Raman (RR) spectrum taken on a quartz substrate spectra for p-SWCNT. A number of SERS and RR spectra were recorded at different parts of the substrate. Comparing the SERS and RR spectra shows a shift in the band positions. A standard deviation of 2.8 cm^{-1} was found in regard to the differences

between the position of the bands in the RR and SERS spectra. Due to this small value of <3 cm^{-1} no correction in regard to estimating the diameter of the SWCNTs according to $\omega_{RBM} = 248/d_t$ was applied. In addition we do not attempt to make any correction in this formula for the presence of the side groups in o and f SWCNTs when calculating the tube diameters for these nanotubes.

The SERS spectra for o-SWCNT and f-SWCNT were recorded using an excitation wavelength of 632 nm (shown in Fig 2). The SERS spectra in the RBM region show a multitude of peaks as evidenced from curve fitting as shown in Fig 2. The SERS spectrum for o-SWCNT has major peaks at 197, 218 and 255 cm^{-1}. The SERS spectrum for f-SWCNT show peaks at 175, 194, 216 and 257 cm^{-1}. Changing the excitation wavelength to 532 nm (see Fig 2), changes also the RBM spectrum as SWCNTs with different chiralities are excited. The spectra show that the o-SWCNT has major peaks at 218 and 255 cm^{-1}, these peaks correspond to tube diameters of 0.88 and 1.03 nm. The background in the SERS spectra makes it difficult to identify additional peaks. The SERS spectrum for f-SWCNT show peaks at 216 and 257 cm^{-1}. These peaks correspond to tube diameters of 0.87 and 1.03 nm. According to the Kataura plot at an excitation wavelength of 532 nm (2.33 eV) RBM peaks between 200 and 275 cm^{-1} arise from metallic nanotubes and those above 275 cm^{-1} from semiconducting tubes [1]. At an excitation wavelength of 632 nm only RBM bands below 225 cm^{-1} belong to metallic nanotubes while the bands above 225 cm^{-1} arise from semiconducting nanotubes. With regard to the peak positions in our RBM SERS spectra for o- and f-SWCNT this means that at 532 nm excitation predominantly metallic nanotubes are excited while a mix of semiconducting and metal nanotubes are excited at 632 nm.

The G band region in the SERS spectra was investigated. The G band region in both Raman and SERS spectra has been extensively studied. In semiconducting nanotubes Lorentzian oscillators are applied to describe the six Raman-active Modes [1]. The modes are assigned to A_{1g}, E_{1g}, and E_{2g} symmetries, where two modes belong to each symmetry type [1]. Studies based on Raman spectroscopy have reported that for semiconducting nanotubes the E_{1g} and A_{1g} modes with displacements along the nanotube axis predicted to occur at c.a. 1590 cm^{-1} cannot be resolved spectrally [1]. In addition the E_{1g} and A_{1g} modes with displacements in the circumferential directions, predicted to occur at 1570 cm^{-1} cannot be resolved, and therefore, these two *G*-band features, which dominate the Raman spectra of semiconducting SWNTs both, contain unresolved E_{1g} and A_{1g} modes. SERS of semiconductor SWNTs recorded on colloidal silver clusters showed band at c.a. 1590 cm^{-1}, 1570 cm^{-1}, and 1550 cm^{-1}, which were assigned to E_{1g} and A_{1g} modes at 1590 cm^{-1} and 1570 cm^{-1} and to E_{2g} modes expected at c.a. 1605 cm^{-1} and 1543 cm^{-1}. In contrast to the semiconducting nanotubes contribution to the SERS spectra from metallic nanotubes are accounted for by Breit-Wigner-Fano (BWF) lineshapes [1]. The reason for the downshift and broadening of the tangential *G* band of metallic SWNTs relative to semiconducting SWNTs has as yet not been explained. The nanotubes studied here are a mixture of metallic and semiconducting nanotubes.

In order to assess the change in spectral features of the SERS spectra in the G band region (shown in Fig 4) we applied a series of fitting to the spectra based on BWF fits, used to fit metallic G- band regions in SERS spectra. The equation used for the BWF fits (as taken from reference 1 is:

$$I(\omega) = I_0 \frac{[1 + (\omega - \omega_{\mathrm{BWF}})/q\Gamma]^2}{1 + [(\omega - \omega_{\mathrm{BWF}})/\Gamma]^2}$$

For 532 nm excitation the band positions for SERS recorded for o-SWCNT are 1590 cm^{-1} at the peak of the G band region and with a BWF fit at 1553 cm^{-1}. The 1/q value for the BWF fit was = -0.34, ω_0 = 1553 cm^{-1} and Γ = 36 cm^{-1}. The band positions for SERS recorded for f-SWCNT are 1591 cm^{-1} at the peak of the G band region and with a BWF fit at 1558 cm^{-1}. The 1/q value for the BWF fit was = -0.25, ω_0 = 1558 cm^{-1} and Γ = 31 cm^{-1}. The SERS spectral features in the G band region recorded at 532 nm are associated with metallic nanotubes with a large G- band expected to arise when metallic nanotubes are present in a SERS spectrum.

The SERS spectra recorded at 632 nm possess features associated with semiconducting nanotubes with large G+ bands and small G- side bands. Two Lorentzian components have been fitted for G+ band and three Lorentzian components have been fitted for G- . Only the most intense peak was used to assign the band position for the G+/G- peaks. The G band region recorded at 632 nm for o- and f-SWCNT are shown in Fig 3. The G+ bands for o- and f-SWCNTs recorded at 632 nm are 1589 and 1587 cm^{-1} while the G- band for o- and f-SWCNTs are both at 1551 and 1552 cm^{-1}.

Comparing the position of the bands in the G+ region shows that for the spectra recorded at 532 and 632 nm shows a shift of $\leq$2 cm^{-1}. While comparing the position of the bands in the G- region shows that for the spectra recorded at 532 and 632 nm shows a shift of $\leq$5 cm^{-1}

Fig 5 shows the SERS spectra for p-SWCNT for reference. Fig 4 shows the SERS spectra for p-SWCNT in the RBM and G band region along with an AFM topography image of the substrates surface. Comparing the band positions in the G band region for all three SWCNTs the G+ band excited at 532 nm positions a variation of $\leq$2 cm^{-1}. The G- band shows a greater change notably for the SERS spectra recorded at 532 nm when comparing all three SWCNTS ie a shift of up to 13 cm^{-1}. Bands in the RBM region shift by 3 or less cm^{-1} when all three SWCNTs are compared. Examination of the D band position showed that at 632 nm excitation all three SWCNTs showed the same band position (1309 cm^{-1})

Studies by Mevellec et al and Gebhardt et al showed in the Raman studies (noting these studies were Raman not SERS studies) that SWCNTs with covalently functionalized chemical groups attached showed changes in RBM frequencies and transition energies dependent upon the both the size of the side group and also the chemical nature of the side group e.g. when oxygen atoms lie close to the tubes a larger shift in transition energy occurs as compared to that of other carbonaceous chains [34,42]. Mevellec et al [34] reported a blue-shift of RBM frequencies for carbon based moieties (example SWCNT-$(CH_2)_{11}$-R) compared to oxygenated moieties (example SWCNT-CO_2(-R)) of c.a. 5 cm^{-1} depending on the substituent. The reason for this shift may arise from removing or adding electrons from or to the tubes, the resonance energy slightly shifts. Mevellec et al when comparing pristine to oxidised to carbonated SWCNTs (which approximate to p, o and f-SWCNTs in our study) showed that for metallic nanotubes noted that after purification with nitric acid and further oxidation that in the Raman spectrum a strong decrease of the low frequency components of the G band was noted, a similar effect was noted using HIPCO SWCNTs. While at the resonant wavelength we used we did not see a change in the intensity of the low frequency modes in the G band, we do see a shift in their frequency. No significant shifts or changes in the G band region for semiconductor SWCNTs were noted in Mevellec's study.

In the RBM region for the metallic tubes the background was too high for bands to be resolved, while for semiconductor nanotubes in the RBM region similar band positions were seen. This is in part agreement with studies by Mevellec et al who reported that for semiconductor nanotubes no significant shift in the RBM region was seen, however for metallic nanotubes, when functionalised a shift in the RBM region was seen, we see a small shift in the RBM band positions for o-SWCNT compared to f-SWCNT.

Evidence for a small change in SERS as a result of adding fluorescence was found ie comparing the SERS spectra of f and o SWCNTs with exception of the G- region were a significant change was observed. It is known that a charge transfer based mechanism for SERS occurs in SWCNTs. The presence or absence of a side group may affect the charge transfer process thereby leading to differences in the resulting SERS spectra. This effect may result in differences in the observed SERS features notably in the G- band region.

4. Conclusion

Changes in the RBM region comparing p,o and f SWCNTs are seen with wavenumber shifts >1.5 and < 3 cm^{-1}, ie a shift greater than the limitation of the instrument. In the G- band a shift (c.a. 5 cm^{-1}) was seen for metallic nanotubes when comparing the three SWCNTs with each other, while no shift was seen in the G+ region (ie > 1.5 cm^{-1}). These results indicate that SERS is broadly in line with Raman studies of chemically altered SWCNTs. The presence of the SERS effect potentially enables for a sensitive (down to the single molecule level) method of sorting between differently functionalised SWCNTs.

It is known that thin silver films can provide SERS enhancements of c.a. 10^{12} for SWCNTS enabling considerable increase in molecule Raman cross section enabling single molecule SERS/SERS studies [31-32]. However, studies of SWCNTs on thin silver films (c.a. 10 nm) can lead to spectral features assigned to partial degradation of carbon nanotubes via nanotube-metal substrate interface, leading to the formation of graphite-like or carbon particles as indicated by the presence of Raman bands of amorphous carbon together with new bands of C_{60}-like molecules. [33]. No such bands are seen here showing no decomposition using thin films of 22 nm.

The presence of side bands eg f-SWCNT (1558 cm^{-1}) is shown to shift the BWF G band significantly compared to the corresponding band position for p-SWCNT (1545 cm^{-1}). It is reported that the type of chain covalently bound to the tubes plays an important role, notably when oxygen atoms lie close to the tubes, inducing a larger shift in transition energy as compared to that of other carbonaceous chains. The BWF G band for o-SWCNT been 1553 cm-1 supports this assertion in that fewer oxygen atoms are present compared to f-SWCNT. The presence of the side group on the SWCNT is reported to affect the DOS of the SWCNT by in particular the presence of electronegative oxygen which causes electron density in the graphine sheet to change. This in turn may via the resonance and SERS effect course the band positions to shift.

These results demonstrate that SERS can see similar effects to normal Raman in regard to band shifts for SWCNTS and its derivatives. The plasmon enhancement mechanism does not change conditions to mask these effects. This indicates that the origin of these shifts are associated with Raman active RBM and G bands are not sensitive to metallic plasmon active substrates. The presence of the SERS effect potentially enables for a sensitive (down to the single molecule level) method of sorting between differently functionalised SWCNTs.

Acknowledgment

The authors acknowledge Science Foundation Ireland (PIYRA 07/YI2/I1052), IRCSET and Intel (postdoctoral fellowship to IK) for support. We acknowledge the support from the Iraq government for their postgraduate studentship for Nebras Al-Alttar. We are grateful to Dr. Kevin Flavin for the o-SWCNTs.

References

1. Carbon Nanotubes, Edited by M.S. Dresselhaus, G. Dresselhaus, P. Avouris, Topics in Applied Physics, 80.

2. J.C. Charlier, Account. Chem. Research, 35 (2002) 1063.

3. J.H. Rice, J.W. Robinson, A. Joujour, R.A. Taylor, R. Oliver, G.A.D. Briggs. Appl Phys Letts, 84(2004) 41101.

4. R. A. Taylor, J.W. Robinson, A. Joujour, R.A. Taylor, R. Oliver, G.A.D. Briggs, Phys. E-Low Dimen. Systems, 21(2004) 285.

5. J.H. Rice, J.P. Galaup, S. Leach, Chem. Phys. 279 (2002) 23

6. J.H. Rice, R. Aures, J.P. Galaup, S. Leach, Chem. Phys. 263 (2001) 401-414

7. R.W. Martin, P.R. Edwards, J.H. Rice, J.W. Robinson, A. Joujour, R.A. Taylor, R. Oliver, G.A.D. Briggs, Phys. Stat. Sol. A., 202 (2005) 372.

8. J.H. Na, J.H. Rice, R.A. Taylor, R. Oliver, G.A.D. Briggs, Appl. Phys. Lett., 86 (2005) 083109.

9. M. Fanti, F. Zerbetto, J.P. Galaup, J.H. Rice, P.R. Birkett, N. Wachter, R. Taylor, J. Chem. Phys., 116 (2002) 7621.

10. J.H. Rice, P.R. Birkett, N. Wachter, J.P. Galaup, R. Taylor, Chem. Phys. Lett., 335 (2001) 553

11. J.H. Na, J.H. Rice, R.A. Taylor, R. Oliver, G.A.D. Briggs, Appl. Phys. Lett., 86 (2005) 123102

12. K. Kneipp, H. Kneipp, M.S. Dresselhaus, S. Lefrant, Phil. Trans. Royal Soc. Series A: 362 (2004) 2361.

13. E. Del Canto, K. Flavin, D. Movia, C. Navio, C. Bittencourt, S. Giordani., Chem Mat., 23(2011) 67.

14. K. Flavin, I. Kopf, E. Del Canto, C. Navio, C. Bittencourt, S. Giordani J. Mat. Chem., 21 (2011) 17881

15. D. Movia, E.D. Canto, S. Giordani, J. Phys. Chem. C, 114 (2010) 18407.

16. D. Movia, E. Del Canto, S. Giordani, Phys. Stat. Solidi B, 246 (2009) 2704.

17. T-J. Park, S. Banerjee, T. Hemraj-Benny, S.S. Wong, J. Mater. Chem. 16 (2006) 141.

18. E. Del Canto, K. Flavin, M. Natali, T. Perova, S. Giordani et al., Carbon 48 (2010) 2815.

19. K. Flavin, K. Lawrence, J. Bartelmess, M. Tasior, C. Navio, C. Bittencourt, D.F. O'Shea, D.M. Guldi, S. Giordani, ACS Nano, 5 (2011) 1198.

20. S. Giordani, J.-F. Colomer, F. Cattaruzza, J. Alfonsi, M. Meneghetti, M. Prato, D. Bonifazi,, Carbon, 47 (2009) 578.

21. T. Fujimori, K. Urita, T. Ohba, H. Kanoh, K. Kaneko, J. Am. Chem. Soc., 132 (2010) 6764.

22. A.J. Stone, D.J. Wales, Chem. Phys. Lett. 128 (1986) 501.

23. N. Al-Alttar, E. Kennedy, I. Kopf, S. Giordani, J.H. Rice. Chem. Phys. Lett., 535 (2012) 146-151

24. F. Lordan, J.H. Rice, B. Jose, R.J. Forster, T.E. Keyes, Appl. Phys. Lett. 99 (2011) 033104-3.

25. F. Lordan, J.H. Rice, B. Jose, R.J. Forster, T.E. Keyes, Appl. Phys. Lett. 97 (2010) 153110.

26. F. Lordan, J.H. Rice, B. Jose, R.J. Forster, T.E. Keyes, J. Phys. Chem. C, 116 (2012) 1784

27. F. Lordan, N. Al-Attar, C. Mallon, J. Bras, G. Collet, R.J. Forster, T.E. Keyes, J.H. Rice. Chem. Phys. Lett. 556 (2013) 158–162

28. S. Damm, N.C. Carville, B.J. Rodriguez, M. Manzo, K. Gallo, J.H. Rice. J. Phys. Chem. C. 116 (2012) 26543–26550

29. N.C. Carville, M. Manzo, S. Damm, M. Castiella, L. Collins, D. Denning, S.A.L. Weber, K. Gallo, J.H. Rice B.J. Rodriguez. ACS Nano, 6 (2012) 7373–7380

30. N. Al-Alttar, E. Kennedy, I. Kopf, S. Giordani, J.H. Rice. Chem. Phys. Lett., 535 (2012) 146-151

31. K. Kneipp, H. Kneipp, M.S. Dresselhaus, S. Lefrant, Phil. Trans. Royal Soc. Series A: 362 (2004) 2361.

32. K. Kneipp, L.T. Perelman, H. Kneipp, V. Backman, A. Jorio, G. Dresselhaus, M.S. Dresselhaus, Phys. Rev. B, 63 (2001) 193411.

33. S. Lefrant, I. Baltog, M. Baibarac, J. Schreiber, O. Chauvet. Phys Rev B, 65 (2002) 235401.

34. J.Y. Mevellec, C. Bergeret, J. Cousseau, J.P. Buisson, C.P. Ewels, S. Lefrant, J. Amer. Chem. Soc., 133 (2011) 16938

35. J. Maultzsch, H. Telg, S. Reich, C. Thomsen, Phys. Rev. B. 72 (2005) 205438.

36. J. Schreiber, P. R. Marcoux, D. Albertini, O. Chauvet, S. Lefrant, AIP Conf. Proc. 633 (2002) 298

37. P.R. Marcoux, J. Schreiber, P. Batail, S. Lefrant, J. Renouard, G. Jacob, D. Albertinib, J.Y. Mevellec, Phys. Chem. Chem. Phys., 4 (2002) 2278

38. P.J. Boul, K. Turner, J. Li, M. X. Pulikkathara, R.C. Dwivedi, E.D. Sosa, Y. Lu, O.V. Kuznetsov, P. Moloney, R. Wilkins, M.J. O'Rourke, V.N. Khabashesku, S. Arepalli, L. Yowell, J. Phys. Chem. C, 113 (2009) 14467

39. J. L. Bahr; J.M. Tour, Chem. Mater., 13 (2001) 3823

40. M.S. Strano, C.A. Dyke, M.L. Usrey, P.W. Barone, M.J. Allen, H.W. Shan, C. Kittrell, R.H. Hauge, J.M. Tour, R.E. Smalley, Science, 301 (2003) 1519

41. G. Hill, J.H. Rice, S.R. Meech, P. Kuo, K. Vodopyanov, M. Reading, nano-Infrared surface imaging using an OPO and an AFM, Optics Letters, 34 (2009) 431–433

42. B. Gebhardt, F. Hof, C. Backes, M. Muller, T. Plocke, J. Maultzsch, C. Thomsen, F. Hauke, A. Hirsch, J. Am. Chem. Soc., 133 (2011) 19459

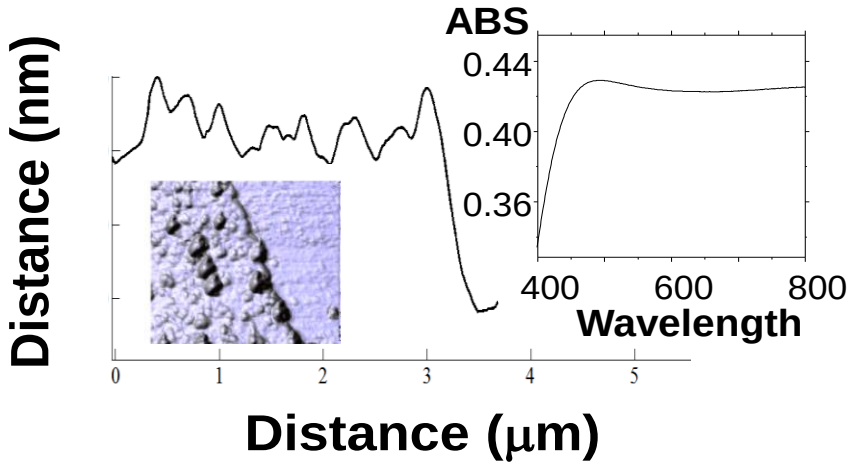

Fig 1. AFM image of the substrate showing also a line scan taken from the AFM image. Shown also is a UV/Vis absorption spectrum of the silver film.

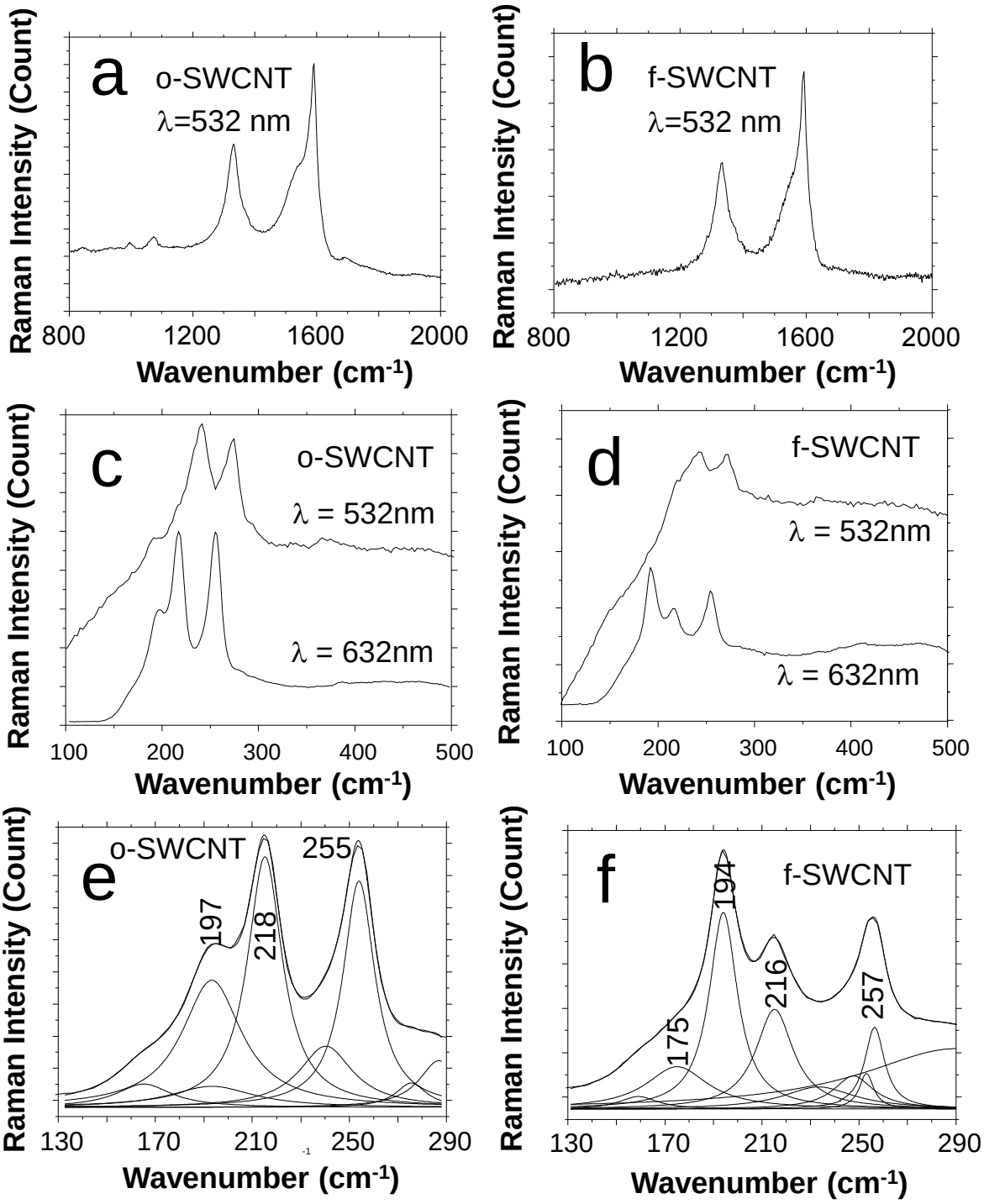

Fig 2. SERS spectra of a) o-SWCNT, b) f-SWCNT, c) RBM spectral region for o-SWCNT, d) RBM spectral region for f-SWCNT, e) and f) SERS spectra recorded in the RBM region recorded at λ_{ex} = 632 nm with Lorenzian curve fits shown. The spectra were recorded at an excitation power of 10 mW before the objective. The spectra were accumulated for 10 seconds.

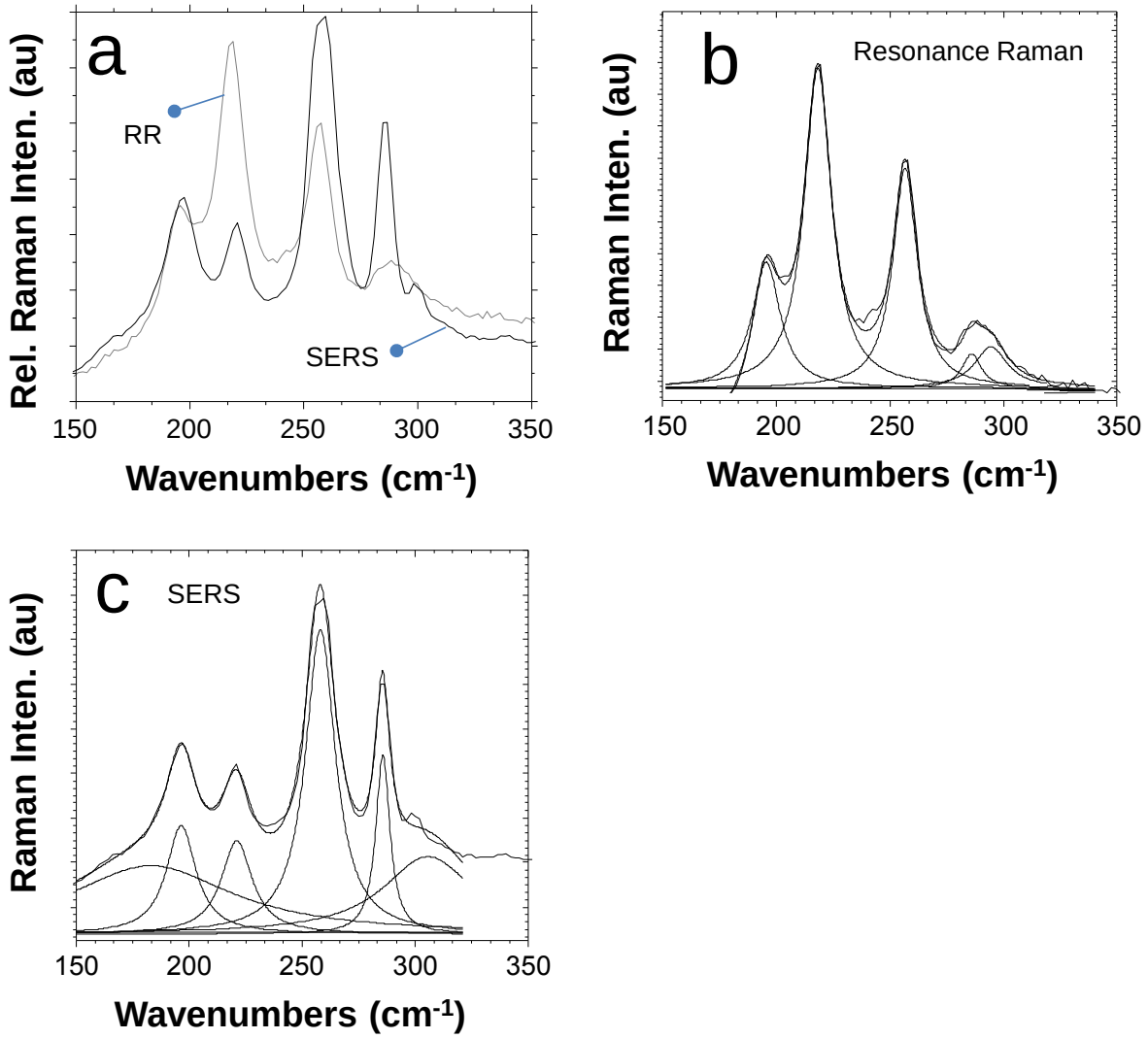

Fig 3. SERS spectra in the RBM band region recorded at 632 nm. a) RR (resonance Raman) spectrum taken on a quartz substrate spectra for p-SWCNT, and a SERS spectrum recorded on a silver film surface 20 nm in thickness. b) RR (resonance Raman) spectrum with Lorrenzian fits and c) SERS spectrum with Lorenzian fits.

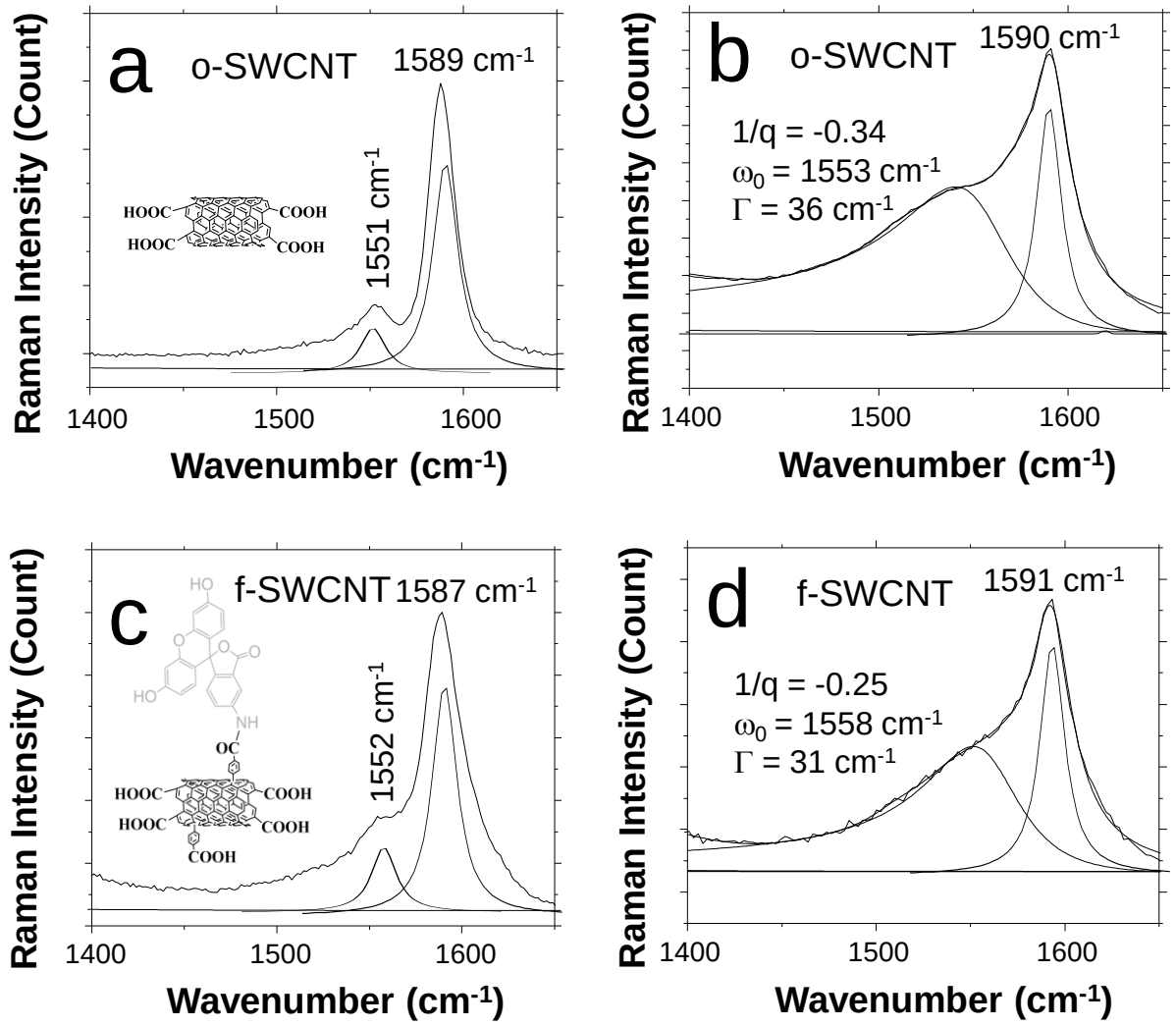

Fig 4. SERS spectra in the G band region. a-c) recorded at 632 nm and b-d) recorded at 532 nm. The spectra were recorded at an excitation power of 10 mW before the objective. The spectra were accumulated for 10 seconds.

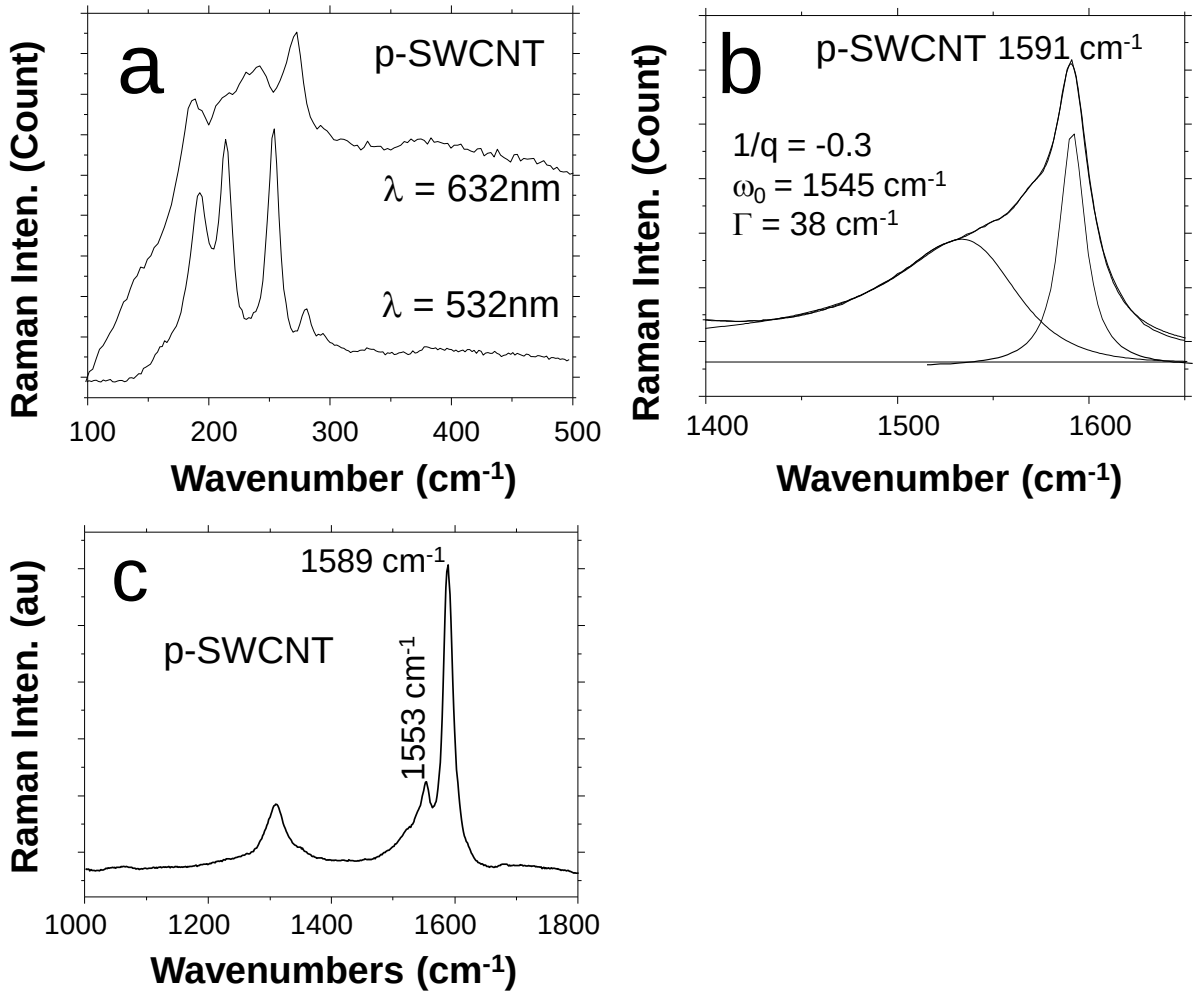

Fig 5. SERS spectra of p-SWCNT a) RBM spectral region, b) G band region at 532 nm, c) G band region at 632 nm.